Perfluorocarbon nanoparticle-mediated platelet inhibition promotes intratumoral infiltration of T cells and boosts immunotherapy

Zaigang Zhou[a,b,1], Baoli Zhang[a,b,1], Wenjing Zai[a,b,1], Lin Kang[a,b], Ahu Yuan[a,b], Yiqiao Hu[a,b,c,2], and Jinhui Wu[a,b,c,2]

[a]State Key Laboratory of Pharmaceutical Biotechnology, Medical School of Nanjing University & School of Life Sciences, Nanjing University, 210093 Nanjing, China; [b]Institute of Drug R&D, Nanjing University, 210093 Nanjing, China; and [c]Jiangsu Provincial Key Laboratory for Nano Technology, Nanjing University, 210093 Nanjing, China

Edited by Hongjie Dai, Department of Chemistry, Stanford University, Stanford, CA, and approved May 6, 2019 (received for review February 6, 2019)

Cancer immunotherapy can stimulate and enhance the ability of the immune system to recognize, arrest, and eliminate tumor cells. Immune checkpoint therapies (e.g., PD-1/PD-L1) have shown an unprecedented and durable clinical response rate in patients among various cancer types. However, a large fraction of patients still does not respond to these checkpoint inhibitors. The main cause of this phenomenon is the limited T-cell infiltration in tumors. Therefore, additional strategies to enhance T-cell trafficking into tumors are urgently needed to improve patients' immune responses. In this study, we screened an array of perfluorocarbon compounds, reporting that albumin-based perfluorotributylamine nanoparticles (PFTBA@Alb) can effectively increase the permeability of tumor blood vessels, and no distinct side effects were found on normal blood vessels. After i.v. administration of PFTBA@Alb, the number of tumor-infiltrating $CD8^+$ and $CD4^+$ T cells showed an obvious rising trend. More important, a striking tumor inhibition rate, reaching nearly 90%, was observed when combining PFTBA@Alb with anti–PD-L1 antibody. These findings suggest that PFTBA@Alb can be regarded as an enhancer for anti–PD-L1 immunotherapy.

immunotherapy | platelet inhibition | immune cell infiltration

Treatment with antiprogrammed death protein-1 (PD-1) or antiprogrammed death ligand 1 (PD-L1) inhibitor cause long-lasting antitumor responses in patients with a variety of cancers, such as breast cancer and colon cancer (1). Nowadays, it has become one of the standard antitumor therapies for patients with cancer (2). However, it is disappointing that only a subset of patients positively respond to these therapies, whereas the majority of patients show resistance to PD-L1 blockade (3). Anti–PD-L1 clinical response to melanoma is closely correlated with the number of $CD8^+$ T cells inside the tumor lesions (4). In this setting, in terms of achieving effective immunotherapy, a therapy that can enhance intratumoral T-cell infiltration would be the most cooperative partner of PD-L1 blockade therapy.

At this time, it is well known that platelets play a vital role in promoting tumor progression, such as by assisting tumor metastasis and decreasing tumor immune sensitivity (5). Moreover, platelets can also reduce the efficacy of cancer chemotherapy by decreasing drug accumulation in tumors (6, 7). This effect is realized by the function of platelets in maintaining the tumor vessel barrier (6–8): Platelets maintain the tumor vessel barrier by releasing soluble factors such as sphingosin-1-phosphate, serotonin, and angiopoietin-1, which then would impede the infiltration of cells, such as red blood cells, into the tumor (8, 9). According to the ability of platelets in limiting cell infiltration in tumors, it is speculated that platelets could also limit T lymphocyte infiltration in tumors through maintaining the tumor vessel barrier (10, 11). Servais et al. (10) proved the assumption that platelet inhibition could prevent carcinogenesis through enhancing T-cell infiltration, leading to restored antitumor immunity. Thus, platelet inhibition could enhance T-cell infiltration in tumors.

At present, platelet depletion can lead to the disrupted tumor vessel barrier, resulting in enhanced tumor vessel permeability (6). This thrombocytopenia-induced tumor vessel barrier disruption appears to be seen in almost all tumors (6). However, current clinically used platelet inhibitors such as aspirin and ticagrelor do not show such effects (5, 12). Existing antiplatelet drugs are all single-targeted platelet inhibitors. Tumors can secrete a variety of factors (e.g., collagen, thrombin, and reactive oxide species) that all can promote platelet activation, leading existing platelet inhibitors being unable to antagonize tumor-induced platelet activation, and being less able to prevent platelets from maintaining tumor vascular integrity (5, 12). Therefore, discovering a platelet inhibitor that can disrupt the tumor vessel barrier is essential for increasing immunotherapy efficacy.

Perfluorocarbons (PFCs) have been widely used in the clinic because of their chemically inert properties (13). Recently, in the course of our research, we happened to find that some PFCs can effectively inhibit platelets and increase the permeability of tumor blood vessels. To find the most ideal PFC possessing the ability to inhibit platelets, we screened 14 different PFC compounds by platelet inhibition ability assay, among which perfluorotributylamine (PFTBA) showed the strongest inhibitory effects. After that, we also screened different nanomaterials of the PFTBA nanoparticle shell (e.g., albumin, phospholipids, and poloxamer), among which

Significance

Trafficking of T cells to tumors is critical for the success of immunotherapy. The success against solid cancers is not as effective as desired owing to limited efficacy in delivering a higher frequency of T cells to the tumor microenvironment. At this time, no useful methods are available to enhance T-cell infiltration in tumors in a short time. New methods that could enhance T-cell trafficking in tumors are urgently in need. Up to now, the role of platelets in limiting T-cell infiltration in tumors is a neglected phenomenon. In our study, for the first time, we proved that perfluorocarbon nanoparticles could promote intratumoral infiltration of T cells via platelet inhibition, resulting in enhanced anti–PD-L1 immunotherapy.

Author contributions: Z.Z., B.Z., A.Y., Y.H., and J.W. designed research; Z.Z., B.Z., W.Z., and L.K. performed research; Z.Z., B.Z., W.Z., and J.W. analyzed data; and Z.Z., B.Z., Y.H., and J.W. wrote the paper.

The authors declare no conflict of interest.

This article is a PNAS Direct Submission.

[1]Z.Z., B.Z., and W.Z. contributed equally to this work.

[2]To whom correspondence may be addressed. Email: huyiqiao@nju.edu.cn or wuj@nju.edu.cn.

This article contains supporting information online at www.pnas.org/lookup/suppl/doi:10.1073/pnas.1901987116/-/DCSupplemental.

Published online May 29, 2019.

we found that PFTBA nanoparticles formed with albumin (PFTBA@Alb) possessed the strongest platelet inhibitory effects. Accordingly, we picked PFTBA@Alb as an optimal platelet inhibitor to further study the effect of platelet inhibition on vascular permeability in detail, and combined with anti–PD-L1 antibody to study the enhanced effects of platelet inhibition on tumor immunotherapy.

Results

At this time, therapeutic interventions targeting immune cells have led to striking improvements in clinical outcomes. To obtain satisfactory immunotherapy responses from existing treatments, a substantial number of tumor infiltrating lymphocytes are critical (4, 11). The more $CD8^+$ T cells infiltrating the tumor site, the better the immunotherapy outcomes (Fig. 1) (14). With a safe and effective method of increasing the infiltration of lymphocytes into poorly immune-responsive tumors, a significant reversion of immunotherapy resistance would be witnessed (Fig. 1).

Screening of a Library of PFC Compounds to Study Their Capacity of Platelet Inhibition. Recently, it has been proven that tumor vascular permeability gradually increases after platelet inhibition or blocking, leading to incremental lymphocyte infiltration. In our previous study, we originally found that some PFC compounds possessed the ability to inhibit platelet function. On the basis of this finding, we further studied in detail the effects on platelet function of 14 PFC compounds (Fig. 2) (15). Among these compounds, we found that PFTBA, perfluorotripentylamine, perfluoroheptane, and perfluorobutyl iodide possessed the most significant platelet inhibition abilities (Fig. 2). Thus, we chose to use PFTBA, which possessed the strongest platelet inhibition effect in vitro, in our following research.

The Platelet Inhibitory Ability of PFTBA Nanoparticles Assembled with Different Materials. PFCs are a class of extremely hydrophobic compounds that cannot be used in vivo without forming nanoparticles. To find the ideal shell material, we constructed three different nanoparticles (PFTBA@Alb, PFTBA@Lip, and PFTBA@Pol) using albumin, phospholipids, and poloxamer, respectively (Fig. 3). The diameters of these nanoparticles were all approximately between 150 and 200 nm, with excellent stability (*SI Appendix*, Fig. S1).

Likewise, we evaluated the inhibiting effects of these nanoparticles on platelet functions through blood clot retraction assay, showing that PFTBA@Alb was the most effective in inhibiting the process of clot retraction (Fig. 3 *A* and *B*). We then further studied their influence on mice platelet adhesion, aggregation, and granule secretion in detail. The results of these additional experiments are consistent with those of the blood clot retraction test: PFTBA@Alb possessed the strongest ability to inhibit platelet adhesion, aggregation, and granule secretion (Fig. 3 *C*–*I*).

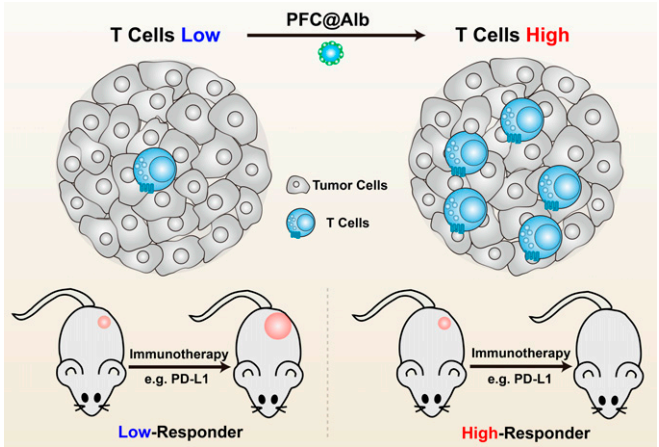

Fig. 1. Schematic illustration of the relationship between the number of T cells and immune response. The tumor infiltrated with more T cells is likely to bring about more effective immune response. Vice versa, less infiltration leads to relatively low response.

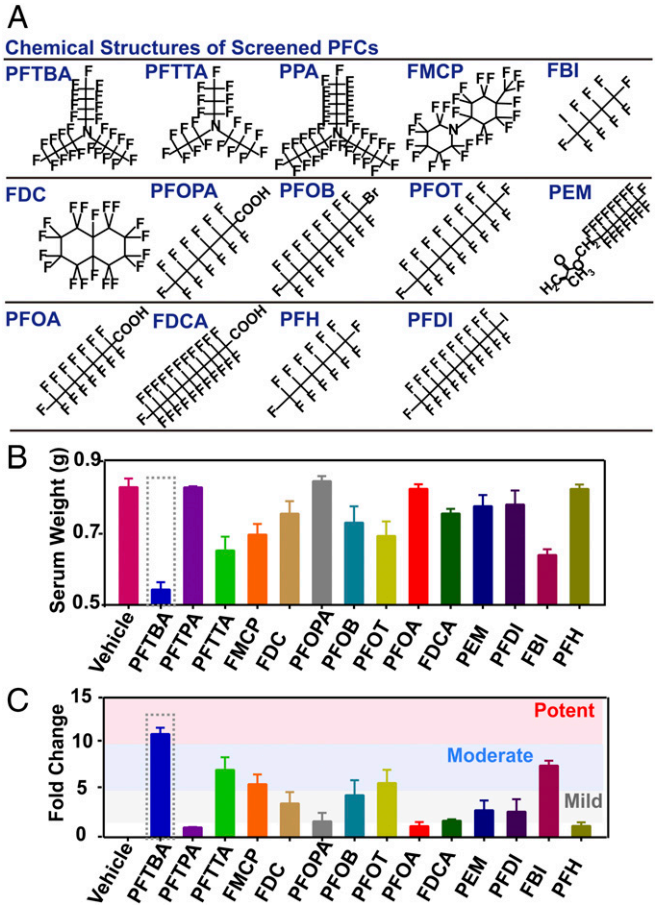

Fig. 2. Screening of the optimal platelet inhibitor among 14 different PFCs by using clot retraction assay. (*A*) The chemical structure of screened PFCs. (*B*) Serum weight at 90 min after different PFC treatment, using clot retraction assay, $n = 3$. (*C*) Fold change of clot weight. Fold change = Clot $Weight_{PFC}$/Clot $Weight_{Vehicle}$. Mild platelet inhibitor, fold change = 1–5; moderate platelet inhibitor, fold change = 5–10; potent platelet inhibitor, fold change > 10 ($n = 3$).

Both angiopietin-1 and 5-HT play principal roles in maintaining the tumor vessel barrier (8). When platelets at the tumor site were effectively inhibited, the integrity of the tumor vessel wall was destroyed, resulting in an enhanced intravascular cell infiltration in tumors (6, 7). Among these nanoparticles, PFTBA@Alb showed the most obvious platelet inhibition effect in mice. This may be because albumin had a higher affinity with platelets than lipid and poloxamer, which may promote the mutual interaction between PFTBA and platelets (16).

Effects of PFTBA@Alb on Tumor-Induced Mice or Human Platelet Activation. We found that PFTBA@Alb can effectively inhibit thrombin-induced platelet activation in mice, including adhesion, aggregation, and granule secretion, in a dose-dependent behavior (*SI Appendix*, Figs. S2–S4). Next, we evaluated the effects of PFTBA@Alb on tumor cells or tumor cell secretion-induced platelet activation, showing that PFTBA@Alb could dose-dependently inhibit the clot retraction induced by CT26 tumor

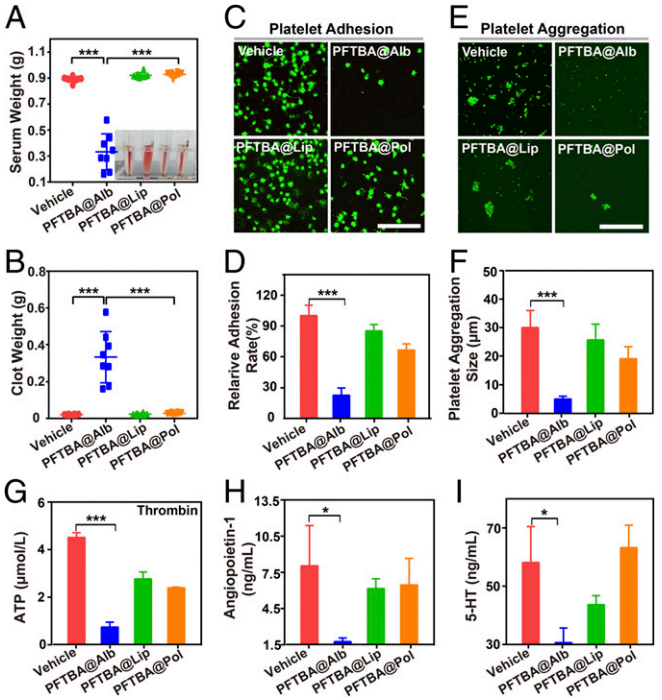

Fig. 3. Effects of different PFTBA nanoparticles on mice platelets. (*A* and *B*) Blood clot retraction test. Clot weight and serum weight at 90 min after mixing with different PFTBA nanoparticles or vehicle (albumin, 1.3 mg/mL; $n = 3$). (*C* and *D*) Representative fluorescent images and quantification of platelet adhesion treated with different PFTBA nanoparticles, platelets were prelabeled with CFSE as green ($n = 4$). (Scale bar: 20 μm.) (*E* and *F*) Representative fluorescent image and quantification of platelet aggregation treated with different PFTBA nanoparticles; platelets were prelabeled with CFSE as green ($n = 4$). (Scale bar: 100 μm.) (*G*) Released platelet granule contents from thrombin-activated platelets ($n = 3$). (*H* and *I*) Released platelet granule contents from activated platelets in vivo ($n = 5$).

cell secretions, whereas ticagrelor cannot (Fig. 4 *A*–*C*). In addition, PFTBA@Alb could also inhibit tumor cell secretions or induced platelet aggregation in mice tumor cells in a dose-dependent manner, whereas ticagrelor was of no effect (Fig. 4 *D*–*F*). As for the platelet secretion test, PFTBA@Albs other than ticagrelor could considerably suppress mice platelets to secrete ATP, angiopoietin-1, and 5-HT. To summarize, PFTBA@Alb possessed the desired mice platelet inhibitory ability, whereas ticagrelor did not.

Different tumor cell types possess different phenotype and cell secretions. Human HT29 colorectal carcinoma cells, human SW480 colon cancer cell secretions, and HepG2 hepatoma carcinoma cell secretions were used to better evaluate the effects of PFTBA@Alb on human platelet function. Results similarly showed that PFTBA@Alb could dose-dependently inhibit platelet activation induced by tumor secretions, while ticagrelor did not have such effect (*SI Appendix*, Figs. S5–S7). Thus, PFTBA@Alb also possessed desired human platelet inhibitory ability whereas ticagrelor did not, meaning that PFTBA@Alb could be used as a potential platelet inhibitor in the near future.

To explore the mechanism of PFTBA@Alb-mediated platelet inhibition, we first detected the concentration of fluorine in or on the platelets. Results showed that fluorine deriving from PFTBA@Alb was located in or on the platelets according to both in vitro and in vivo experiments (*SI Appendix*, Fig. S8 *A* and *B*). To better investigate the accurate location of PFTBA@Alb in platelets, coumarin and dil were used to label PFTBA@Alb and the platelet membrane, respectively. Results indicated that PFTBA@Alb mainly adsorbed on the surface of platelets other than being endocytosed into the cytoplasm (*SI Appendix*, Fig. S8*C*). Moreover, by analyzing the surface morphology of platelets, we found that the platelets treated in vitro by PFTBA@Alb were in an inactive state, whereas platelets deformed and stretched out a parapodium, showing active cell morphology, in the absence of PFTBA@Alb (*SI Appendix*, Fig. S8*D*). On the basis of the above results, we hypothesized that PFTBA adhered to the platelet membrane and further blocked platelet activation pathways leading to platelet inhibition. To confirm this, we chose three different platelet activators, which target three different platelet activation sites, including ADP (P2Y1 and P2Y12 agonist), collagen (GPVI agonist), and thrombin (PAR agonist) (17). As expected, the results revealed that with adsorbed PFTBA@Alb on the platelet membrane, ATP released from platelet granules was significantly inhibited under the stimulation of these platelet activators, including ADP, collagen and thrombin (*SI Appendix*, Fig. S8 *E*–*G*). Thus, the mechanism of PFTBA@Alb-mediated platelet inhibition may be a result of PFTBA@Alb adsorbing on the surface of platelets, covering platelet-activating targets (18).

We also evaluated the effects of PFTBA@Alb on serum platelet numbers and platelet distribution in tumors. Results showed that blood platelet numbers were obviously decreased after PFTBA@Alb treatment, whereas the number of serum red blood cells (RBCs) was not influenced (*SI Appendix*, Fig. S9). Meanwhile, the distribution of CFSE-labeled platelets in tumors was also significantly reduced at 24 h (*SI Appendix*, Fig. S10). Thus, PFTBA@Alb could not only inhibit platelet activation but also partly deplete the platelets in the tumors.

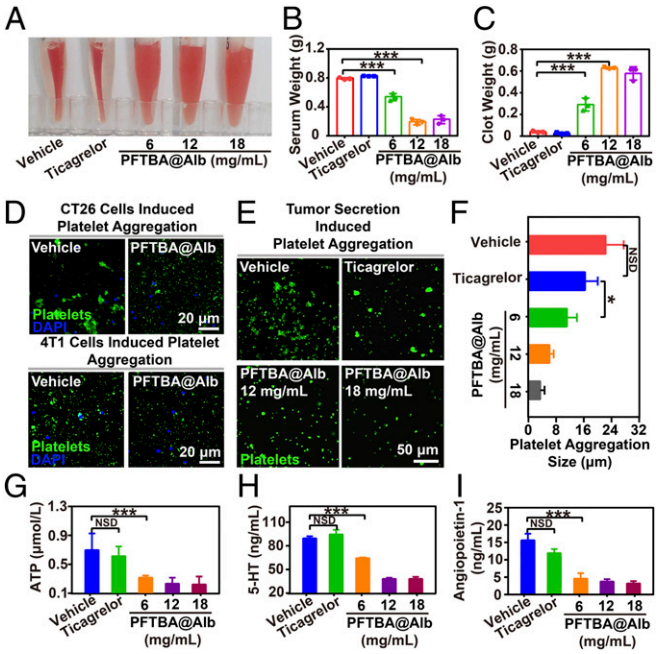

Fig. 4. Effects of PFTBA@Alb on mice platelet function in the presence of tumor cells or tumor cell secretions. (*A*) Representative photos of clot retraction test induced by the hybrid platelet activator (CT26 tumor cell secretions, thrombin, and collagen). (*B* and *C*) Quantification of the clot weight and serum weight of clot retraction test at 90 min after mixing with different concentrations of PFTBA@Alb or ticagrelor (40 μg/mL) or vehicle (albumin, 1.3 mg/mL; $n = 3$). (*D* and *E*) Representative fluorescent images of platelet aggregation induced by CT26 or 4T1 tumor cell or CT26 tumor cell secretions after treating with PFTBA@Alb. Platelets were prelabeled with CFSE. (*F*) Quantification of the size of platelet aggregation induced by tumor cell secretions after treating with different concentrations of PFTBA@Alb ($n = 3$). (*G*–*I*) Platelet granule secretions (ATP, 5-HT, and angiopoietin-1) induced by tumor cell secretions after treating with ticagrelor or different concentrations of PFTBA@Alb.

Effects of PFTBA@Alb on Tumor Vessel Permeability. In general, 5-HT and angiopoietin-1 loaded in platelet granules are key sustainers of lower tumor vascular permeability (8). With the decline of 5-HT and angiopoietin-1 level in serum, the tumor vessel permeability would be enhanced (6). As we previously proved, PFTBA@Alb could effectively inhibit the secretion of 5-HT and angiopoietin-1 by preventing platelets from activation (Figs. 3 and 4). Thus, we speculated that PFTBA@Alb could increase the permeability of tumor blood vessels.

To further visualize the effect of PFTBA@Alb on tumor vessel integrity, dextran (2,000 kDa, ∼30 nm) and Evans blue were used. Results indicated that only few fluorescent dyes distributed inside the tumor when either dextran or Evans blue alone was applied (Fig. 5*A*). When coadministered with PFTBA@Alb, the accumulation of dextran and Evans blue in tumors was obviously increased, whereas that was not the case with coadministration with ticagrelor (Fig. 5*A* and *SI Appendix*, Fig. S11). If additional platelets were reperfused into mice 1 h after PFTBA@Alb treatment, the ability of PFTBA@Alb to increase the accumulation of dextran and Evans blue were inhibited, meaning that increased tumor vessel permeability was mediated to some extent by platelet inhibition (Fig. 5*A*). Meanwhile, it is also worth noting that PFTBA@Alb had an effect neither on dextran (Mw 70 kDa and 2,000 kDa) permeation or Evans blue distribution in normal tissues (*SI Appendix*, Fig. S12).

The enhancement of tumor vessel permeability seen with the application of PFTBA@Alb may be caused by the reasons given here. Many platelets are located in the tumor site and are in a continuously activated state. Once the platelets are inhibited in vessels, the tumor-associated platelets will be rapidly affected to a great extent, and the tumor vessels will exhibit symptoms of platelet inhibition. Nevertheless, normal tissue blood vessels would not be affected by moderate platelet inhibition unless there is almost total platelet depletion (5, 8).

Effects of PFTBA@Alb on Red Blood Cell and T-Cell Distribution in Tumors. After that, we evaluated the effects of PFTBA@Alb on erythrocyte infiltration. Results showed that the number of RBCs were enormously increased in CT26 tumors in time-dependent behavior after PFTBA@Alb treatment (Fig. 5 *C* and *D*). In comparison with normal tissues, PFTBA@Alb had no effects on RBCs accumulation (*SI Appendix*, Fig. S13).

Because RBCs can infiltrate tumors via a tumor vessel barrier disrupted by PFTBA@Alb, it can be questioned whether the intratumoral infiltration of lymphocytes could be augmented in the same manner (19). To answer this question, we observed the accumulation of i.v. injected CFSE-labeled lymphocytes in tumors (Fig. 5*E*). It is interesting to note that PFTBA@Alb could also notably enhance lymphocyte infiltration in tumors. After excess platelet reperfusion, the ability of PFTBA@Alb to enhance lymphocyte cell infiltration in tumors can be inhibited (Fig. 5*E*).

Flow cytometry assay was employed to further accurately quantify $CD4^+$ and $CD8^+$ T-cell infiltration in tumors. With the assistance of PFTBA@Alb, the infiltration of T cells within the tumors was significantly enhanced in a dose-dependent and time-dependent manner (Fig. 5 *F–I* and *SI Appendix*, Figs. S14–S15). Likewise, additional platelet reperfusion could inhibit the ability of PFTBA@Alb to enhance T-cell trafficking in tumors, indicating that the increased T-cell infiltration in tumors was mediated by the platelet-inhibiting capacity of PFTBA@Alb to some degree (Fig. 5 *F–I*).

Recently, several works also proved that attenuation of tumor hypoxia is able to promote the intratumoral infiltration of T cells (20–22). Thus, tumor hypoxia attenuation may also work to some degree in PFTBA@Alb-enhanced intratumoral infiltration of T cells, as PFTBA possessed an ideal physical oxygen binding ability. To evaluate this concept, intratumoral injection of PFTBA@Alb was conducted. Results showed that oxygen carried by PFTBA@Alb was not able to enhance T-cell infiltration (*SI Appendix*, Fig. S16). It was also indicated that PPA@Alb with a weak platelet inhibition ability could not enhance the intratumoral infiltration of T cells as well as the PFTBA@Alb with ideal platelet inhibition ability did (*SI Appendix*, Fig. S16). Thus, effective platelet inhibition other than tumor hypoxia attenuation resulted in the improved intratumoral infiltration of T cells mediated by PFTBA@Alb.

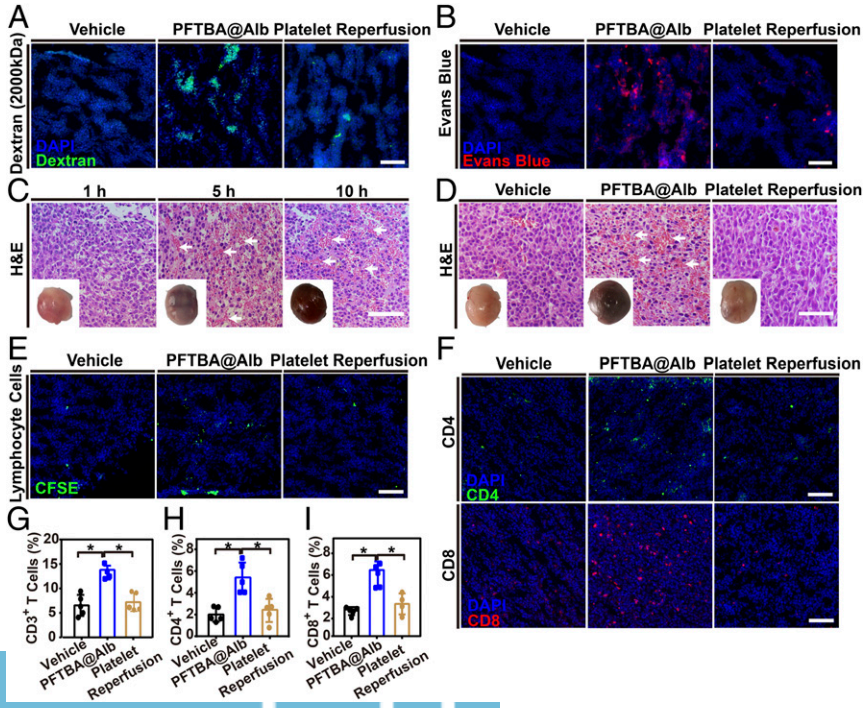

Fig. 5. Effects of PFTBA@Alb on tumor vessel permeability and cell infiltration in CT26-bearing mice. (*A* and *B*) Representative fluorescence images of tumor slices after Dextran (2,000 kDa, green) or Evans blue (red) administration in the presence or absence of PFTBA@Alb, (Scale bar: 100 μm.) (*C* and *D*) H&E stained tumor slices and tumor photos at different times postadministration of PFTBA@Alb in the presence or absence of platelet transfusion. White arrows denote RBCs. (Scale bar: 100 μm.) (*E*) Representative fluorescent images of lymphocyte cell infiltration in tumors. Lymphocyte cells were isolated from spleen and prelabeled with CFSE (green), then reinjected i.v. into mice. Images were taken at 24 h postinjection. (Scale bar: 100 μm.) (*F*) Representative fluorescent images of $CD4^+$ and $CD8^+$ T-cell infiltration after PFTBA@Alb administration. (Scale bar: 100 μm.) (*G–I*) Quantification of the percentage of $CD4^+$ and $CD8^+$ T-cell infiltration in total cells distributed in tumors by flow cytometry assay ($n = 5$).

Enhanced Effects of PFTBA@Alb Combined Anti–PD-L1 Immunotherapy in CT26 Tumors. Furthermore, we speculated that PFTBA@Alb could increase the efficacy of immunotherapy via improved tumor T-cell infiltration. To confirm our speculation, we combined PFTBA@Alb with anti–PD-L1 antibody to explore the effect of PFTBA@Alb on immunotherapy efficacy. Results revealed that PFTBA@Alb itself did not have any antitumor effect (Fig. 6 and *SI Appendix*, Fig. S17). However, when it was used as a cotreatment with anti–PD-L1 antibody, the tumor growth rate (Fig. 6*A*) and tumor weight (Fig. 6*B*) were both significantly decreased compared with those of anti–PD-L1 antibody treatment alone. These results indicated that a high tumor inhibition rate reached nearly 90% after the use of PFTBA@Alb combined with anti–PD-L1 antibody (Fig. 6*A*). Meanwhile, the mean tumor weight of the combination group was only 10% of the vehicle group, and was nearly 20% of the average tumor weight of the anti–PD-L1 group (Fig. 6*B*). Moreover, the necrosis and apoptosis of tumor cells after combination therapy were significantly increased (*SI Appendix*, Fig. S18).

More important, there were no significant changes in body weight and normal tissue cell morphology after PFTBA@Alb administration (Fig. 6*C* and *SI Appendix*, Fig. S19), indicating that PFTBA@Alb possessed good biocompatibility in vivo.

Cytokines (e.g., IFN-γ, IL-6, and TNF-α) are important indicators to predict and evaluate immune responses (23). As our results indicate, the expression of IFN-γ, IL-6, and TNF-α in the tumor and serum were rapidly increased after coadministration of PFTBA@Alb and anti–PD-L1 antibody (Fig. 6 *D–F* and *SI Appendix*, Fig. S20), meaning that tumor immune sensitivity was effectively enhanced. Moreover, the infiltration of $CD45^+$ lymphocytes, $CD4^+$ T cells, and $CD8^+$ T cells in the tumors were all enhanced after PFTBA@Alb treatment (Fig. 6 *G–J*). Apart from this, the number of IFN-γ^+ $CD8^+$ and Granzyme B^+ $CD8^+$ T cells in CT26 tumors were both increased after cotreating PFTBA@Alb with anti–PD-L1 antibody, indicating that PFTBA@Alb treatment could also improve the activity and multifunctionality of $CD8^+$ T cells in vivo (*SI Appendix*, Fig. S21). Therefore, PFTBA@Alb could be regarded as a potential and novel type of clinical anti–PD-L1 immunotherapy enhancer.

Enhanced Effects of PFTBA@Alb Combined with Anti–PD-L1 Immunotherapy in B16F10 Tumors. To evaluate the universality of PFTBA@Alb in enhancing tumor immune sensitivity in other tumor types, the B16F10 tumor model was selected. Results also showed that the infiltration of $CD3^+$, $CD4^+$, and $CD8^+$ T cells in the B16F10 tumors were all enhanced after PFTBA@Alb treatment (*SI Appendix*, Fig. S22). Meanwhile, the number of IFN-γ^+ $CD8^+$ and Granzyme B^+ $CD8^+$ T cells in B16F10 tumors were both increased after PFTBA@Alb treatment, meaning that the number of effective $CD8^+$ T cells was also enhanced after PFTBA@Alb treatment (*SI Appendix*, Fig. S22). Moreover, it was revealed that tumor growth rate was obviously inhibited and tumor weight decreased when PFTBA@Alb was coadministered with anti–PD-L1 antibody (*SI Appendix*, Fig. S23). Above all, PFTBA@Alb is a potential clinical anti–PD-L1 immunotherapy enhancer that is suitable for multiple tumor types.

Discussion

In our study, we proved that PFTBA@Alb was able to inhibit platelets, which could break tumor vessel barriers and further significantly enhance their permeability because of the critical role of platelets in maintaining tumor vessel integrity (24). Meanwhile, PFTBA@Alb had no effect on normal tissue blood vessels

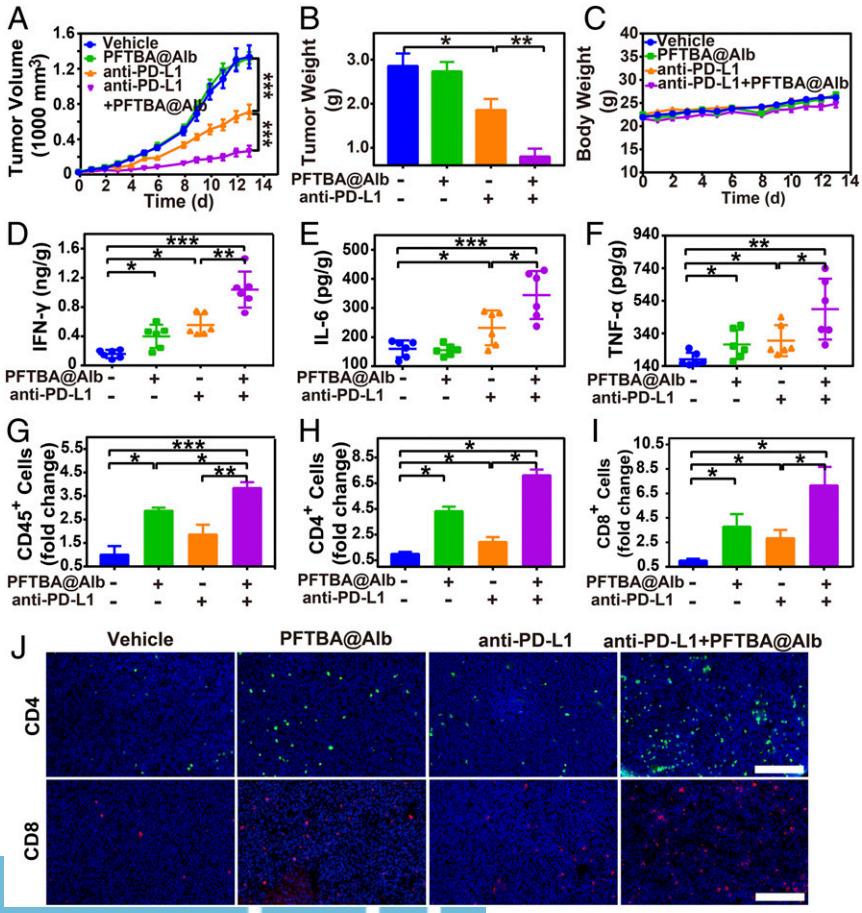

Fig. 6. Effects of PFTBA@Alb on anti–PD-L1 antibody-mediated immunotherapy. (*A*) Tumor growth curves of CT26 tumor-bearing mice ($n = 8$). (*B*) Tumor weight at day 13 posttreatments ($n = 8$). (*C*) Body weight curves. (*D–F*) Protein levels of IFN-γ, IL-6, and TNF-α in CT26 tumor at day 13 posttreatments. (*G–I*) Fold change of the $CD45^+$ lymphocytes, tumor-infiltrating $CD4^+$ and $CD8^+$ T cells in all the cells in CT26 tumors compared with the vehicle group (albumin, 3.2 g/kg). (*J*) Representative images of the immune fluorescence staining of the intratumor-infiltrating $CD4^+$ T cells (green) and $CD8^+$ T cells (red). (Scale bar: 100 μm.)

because well-arranged normal blood vessel endothelial cells do not need activated platelets to maintain the blood vessel barrier (6). When anti–PD-L1 antibodies were cotreated with PFTBA@Alb, the efficacy of combined immunotherapy was considerably amplified as a consequence of disrupted tumor vessel barriers and enhanced infiltration of T cells into tumors.

We next evaluated whether existing single-target platelet inhibitors could also disrupt tumor vessel barriers as PFTBA@Alb did. Results showed that clinically used small molecular platelet inhibitors such as ticagrelor could enhance neither the tumor vessel permeability nor the T-cell infiltration in tumors (*SI Appendix*, Figs. S11 and S24). This phenomenon may a result of tumor cells secreting a variety of active molecules such as ROS, thrombin, and collagen, which could then induce the activation of platelets in the tumor vessels by different platelet activation pathways. Undoubtedly, tumor-associated platelets could not be simply inhibited by a single target inhibitor (e.g., ticagrelor). As far as we know, no platelet inhibitors in the clinic are now available to enhance the efficacy of immunotherapy through enlarged T-cell infiltration, as PFTBA@Alb does.

At this time, transporting T cells to the tumor microenvironment is essential for the success of cancer immunotherapies, especially in adoptive T-cell immunotherapy (25). Although adoptive T-cell therapy has already achieved remarkable responses in patients with hematologic malignancy, the outcome of solid cancers has been seriously limited and unsatisfactory (9). The process of T-cell trafficking to the tumor microenvironment is highly dynamic, involving a series of distinct processes, including rolling, adhesion, extravasation, and chemotaxis (9, 26). One of the major challenges of adoptive T-cell therapy is to overcome aberrant tumor vasculature barrier so as to deliver a higher frequency of T cells into the tumor microenvironment (9, 27). In our study, we found that PFTBA@Alb could effectively promote the CFSE-labeled lymphocyte distribution in tumors to simulate the T-cell infiltration process of adoptive cell therapy (Fig. 5 *E*–*I*). Therefore, we believed that PFTBA@Alb can enhance the efficacy of current adoptive T-cell therapy.

In this study, for the purpose of delivering extremely hydrophobic PFTBA in vivo, albumin was picked out as the ideal drug carrier. It is well known that albumin-based nanoparticles have been widely used in the clinic, like Abraxane (28). Of critical importance, Fluosol-43 (a PFTBA nanoemulsion) with superior biosafety has been already approved by the US Food and Drug Administration as an oxygen carrier to improve myocardial oxygenation (29, 30). Our results also proved that PFTBA@Alb had no adverse effects on normal tissues of both Balb/C and C57BL/6 mice (*SI Appendix*, Figs. S25 and S26). Therefore, PFTBA@Alb could be a promising way to enhance the efficacy of anti–PD-L1 immunotherapy.

Conclusion. Relatively tight vascular barrier and the consequent inadequate immunocompetent cell infiltration limit the overall efficacy of immunotherapy. In this study, PFTBA@Alb could significantly disrupt tumor vessel barriers through effective platelet inhibition. By doing this, the immune cell infiltration in tumors was significantly enhanced. These dramatically enhanced the sensitivity of tumors to the current immunotherapies, especially anti–PD-L1 immunotherapy. All materials that constitute PFTBA@Alb, including albumin and PFTBA, have already been widely used in the clinic. Thus, PFTBA@Alb could be used as a method for enhancing the efficacy of immunotherapy with great prospects of clinical use.

Methods

The effects of PFTBA@Alb on mice or human platelets function were studied. The effects of PFTBA@Alb on tumor vessel permeability, T-cell infiltration, and immunotherapy efficacy were studied in CT26 or B16F10 tumors. For additional information regarding the platelet function inhibition screening assay, treatment protocols, and statistical analysis, see *SI Appendix, Materials and Methods*. Statistical analysis was performed via one-way ANOVA test. Meanwhile, post hoc analysis was performed using the Wilcoxon rank sum test with a Bonferroni correction if needed. $*P < 0.05$ was considered statistically significant; $**P < 0.01$ and $***P < 0.001$ were extremely significant. NSD, no significant difference, $P > 0.05$.

ACKNOWLEDGMENTS. This paper was supported by the National Key R&D Program of China (2017YFA0205400) and the National Natural Science Foundation of China (No. 31872755, 81872811). This project was also supported by the Central Fundamental Research Funds for the Central Universities (021414380447, 02141480608201).

1. J. R. Brahmer *et al.*, Safety and activity of anti-PD-L1 antibody in patients with advanced cancer. *N. Engl. J. Med.* **366**, 2455–2465 (2012).
2. K. M. Mahoney, P. D. Rennert, G. J. Freeman, Combination cancer immunotherapy and new immunomodulatory targets. *Nat. Rev. Drug Discov.* **14**, 561–584 (2015).
3. D. S. Chen, I. Mellman, Elements of cancer immunity and the cancer-immune set point. *Nature* **541**, 321–330 (2017).
4. C. Robert *et al.*; KEYNOTE-006 Investigators, Pembrolizumab versus ipilimumab in advanced melanoma. *N. Engl. J. Med.* **372**, 2521–2532 (2015).
5. M. Haemmerle, R. L. Stone, D. G. Menter, V. Afshar-Kharghan, A. K. Sood, The platelet lifeline to cancer: Challenges and opportunities. *Cancer Cell* **33**, 965–983 (2018).
6. B. Ho-Tin-Noé, T. Goerge, S. M. Cifuni, D. Duerschmied, D. D. Wagner, Platelet granule secretion continuously prevents intratumor hemorrhage. *Cancer Res.* **68**, 6851–6858 (2008).
7. M. Demers, D. D. Wagner, Targeting platelet function to improve drug delivery. *OncoImmunology* **1**, 100–102 (2012).
8. B. Ho-Tin-Noé, T. Goerge, D. D. Wagner, Platelets: Guardians of tumor vasculature. *Cancer Res.* **69**, 5623–5626 (2009).
9. C. Y. Slaney, M. H. Kershaw, P. K. Darcy, Trafficking of T cells into tumors. *Cancer Res.* **74**, 7168–7174 (2014).
10. L. Servais *et al.*, Platelets contribute to the initiation of colitis-associated cancer by promoting immunosuppression. *J. Thromb. Haemost.* **16**, 762–777 (2018).
11. S. L. Topalian *et al.*, Safety, activity, and immune correlates of anti-PD-1 antibody in cancer. *N. Engl. J. Med.* **366**, 2443–2454 (2012).
12. M. L. O'Donoghue *et al.*, Pharmacodynamic effect and clinical efficacy of clopidogrel and prasugrel with or without a proton-pump inhibitor: An analysis of two randomised trials. *Lancet* **374**, 989–997 (2009).
13. J. G. Riess, Perfluorocarbon-based oxygen delivery. *Artif. Cells Blood Substit. Immobil. Biotechnol.* **34**, 567–580 (2006).
14. P. C. Tumeh *et al.*, PD-1 blockade induces responses by inhibiting adaptive immune resistance. *Nature* **515**, 568–571 (2014).
15. P. M. Nair *et al.*, Platelet aggregation is important for efficient clot retraction. *Blood* **130**, 1122 (2017).
16. B. Sivaraman, R. A. Latour, Time-dependent conformational changes in adsorbed albumin and its effect on platelet adhesion. *Langmuir* **28**, 2745–2752 (2012).
17. Z. Li, M. K. Delaney, K. A. O'Brien, X. Du, Signaling during platelet adhesion and activation. *Arterioscler. Thromb. Vasc. Biol.* **30**, 2341–2349 (2010).
18. V. V. Tuliani, E. A. O'Rear, B. M. Fung, B. D. Sierra, Interaction between erythrocytes and a perfluorochemical blood substitute. *J. Biomed. Mater. Res.* **22**, 45–61 (1988).
19. G. P. Downey *et al.*, Retention of leukocytes in capillaries: Role of cell size and deformability. *J. Appl. Physiol.* **69**, 1767–1778 (1990).
20. Y. Chao *et al.*, Combined local immunostimulatory radioisotope therapy and systemic immune checkpoint blockade imparts potent antitumour responses. *Nat. Biomed. Eng.* **2**, 611–621 (2018).
21. G. Yang *et al.*, Hollow MnO_2 as a tumor-microenvironment-responsive biodegradable nano-platform for combination therapy favoring antitumor immune responses. *Nat. Commun.* **8**, 902 (2017).
22. X. Song, L. Feng, C. Liang, K. Yang, Z. Liu, Ultrasound triggered tumor oxygenation with oxygen-shuttle nanoperfluorocarbon to overcome hypoxia-associated resistance in cancer therapies. *Nano Lett.* **16**, 6145–6153 (2016).
23. Q. Chen *et al.*, Photothermal therapy with immune-adjuvant nanoparticles together with checkpoint blockade for effective cancer immunotherapy. *Nat. Commun.* **7**, 13193 (2016).
24. B. Ho-Tin-Noé, M. Demers, D. D. Wagner, How platelets safeguard vascular integrity. *J. Thromb. Haemost.* **9** (suppl. 1), 56–65 (2011).
25. H. J. Jackson, S. Rafiq, R. J. Brentjens, Driving CAR T-cells forward. *Nat. Rev. Clin. Oncol.* **13**, 370–383 (2016).
26. J. A. Craddock *et al.*, Enhanced tumor trafficking of GD2 chimeric antigen receptor T cells by expression of the chemokine receptor CCR2b. *J. Immunother.* **33**, 780–788 (2010).
27. C. H. June, S. R. Riddell, T. N. Schumacher, Adoptive cellular therapy: A race to the finish line. *Sci. Transl. Med.* **7**, 280ps7 (2015).
28. L. Meng *et al.*, Facile deposition of manganese dioxide to albumin-bound paclitaxel nanoparticles for modulation of hypoxic tumor microenvironment to improve chemoradiation therapy. *Mol. Pharm.* **15**, 447–457 (2018).
29. L. H. Young, C. C. Jaffe, J. H. Revkin, P. H. McNulty, M. Cleman, Metabolic and functional effects of perfluorocarbon distal perfusion during coronary angioplasty. *Am. J. Cardiol.* **65**, 986–990 (1990).
30. E. Maevsky *et al.*, Clinical results of perftoran application: Present and future. *Artif. Cells Blood Substit. Immobil. Biotechnol.* **33**, 37–46 (2005).